Table 1. Effect of hepatectomy on the incorporation of L-methionine-methyl-C^{14} into maternal and fetal serum globulins. Dose: 10^6 count/min, 37 μg per mother.

Av. fetal wt. (g)	Percentage hepatectomy	Specific activity (count/min per milligram of globulins)	
		Mother	Fetus
2.6	69	34	0
3.1	68	28	41
3.1	Sham control	46	64
	Intact control	41	56

serve as controls. In a second group of experiments the amino acid was injected directly into the fetus *in utero*. The fetuses were located and injected intraperitoneally through the uterine wall with the amino acid. Three hours later the fetal and maternal bloods were obtained. The fetuses showed spontaneous movement when bled. The serums were separated immediately and either processed or frozen at −20°C. The serum proteins were precipitated and washed by the procedure of Zamecnik *et al.* (*4*). Serum albumins of several species are soluble in a number of organic solvents after precipitation with trichloroacetic or other acids (*5*). This property was used to separate the serum albumin from the serum globulins during the washing. The supernatant fluid from the first ethanol wash was saved and either it was exhaustively dialyzed against distilled water or the ethanol was evaporated *in vacuo*. The dialyzed material was electrophoretically homogeneous and showed the mobility of albumin but had at least two quantitatively minor contaminants evident upon immunoelectrophoresis. The albumin samples were prepared for counting by reprecipitation in trichloroacetic acid and heating to 95°C for 15 minutes, which rendered the albumin insoluble in ethanol. The washed precipitates were dissolved in 0.1*N* NaOH and counted in a liquid scintillation counter with the solvent system described by Bray (*6*). Protein concentrations were measured by the procedure of Lowry *et al.* (*7*).

Table 1 presents the specific activities of the fetal and maternal globulins when L-methionine-methyl-C^{14} was injected by tail vein into intact, sham-operated, and partially hepatectomized pregnant rats. The specific activity of the fetal serum globulin was variable and the effect of hepatectomy small. Similar results were obtained when the incorporation of L-leucine into serum albumin and globulins was studied by this method.

Table 2 shows the incorporation of amino acids into the serum proteins of the mother and fetus when the fetuses were injected *in utero*. The consistent finding of a much higher specific activity in the fetal serum proteins than in the corresponding maternal proteins indicates that serum albumin and at least some of the serum globulins are formed by the fetus at this stage of gestation. The marked difference between the two methods of injection may be attributed to the much larger pool of amino acid with which the labeled amino acid is diluted when it is injected directly into the maternal circulation. Further, the transplacental concentration gradient of free amino acids indicates a limited passage of amino acids from the fetus to the mother (*8*). Therefore, an amino acid injected into the fetus would be preferentially utilized by the fetus. Our findings regarding the effect of the route of injection on the utilization of amino acids by mother and fetus are in agreement with those of Kulangara and Schjeide (*9*) in rabbits, although different methods of expressing the results were used in the two studies (*10*).

Table 2. Incorporation of labeled amino acids into serum proteins by the rat fetus. Abbreviations: *A*, albumin; *G*, globulins.

Av. fetal wt. (g)	Fetuses (No.)	Fraction	Specific activity (count/min per milligram of protein)	
			Mother	Fetus
L-methionine-methyl-C^{14} (dose: 10^5 count/min, 3.7 μg per fetus)				
5.3	9	G	13	160
L-leucine-U-C^{14} (dose: 8.06 × 10^4 count/min, 0.52 μg per fetus)				
2.6	18	A	55	484
		G	47	439
3.7	13	A	33	274
		G	18	287
4.2	11	A	53	193
		G	24	183
L-leucine-U-C^{14} (dose: 2.02 × 10^5 count/min, 0.25 μg per fetus)				
3.3	5	A	34	846
		G	29	912
3.8	9	A	68	771
		G	56	803
3.9	13	A	113	822
		G	110	844
4.2	11	A	77	474
		G	52	446
4.6	11	A	78	417
		G	49	418

P. C. KELLEHER
C. D. KENYON
C. A. VILLEE

Department of Biological Chemistry, Harvard Medical School, and Research Laboratories, Boston Lying-in Hospital, Boston, Massachusetts

References and Notes

1. F. Galatius-Jensen, *Proc. Sixth Europ. Congr. Haematol.* **269** (1957); A. R. Rausen, P. S. Gerald, L. K. Diamond, *Nature* **191**, 717 (1961); *ibid.* **192**, 182 (1961).
2. J. Dancis, N. Braverman, J. Lind, *J. Clin. Invest.* **36**, 398 (1957); ——— and M. Shafran, *ibid.* **37**, 1093 (1958).
3. P. C. Kelleher and C. A. Villee, *Biochim. Biophys. Acta* **59**, 252 (1962).
4. P. C. Zamecnik, R. B. Loftfield, M. L. Stephenson, J. M. Steele, *Cancer Res.* **11**, 592 (1951).
5. A. Korner and J. Debro, *Nature* **178**, 1067 (1956); G. W. Schwert, *J. Am. Chem. Soc.* **79**, 139 (1957).
6. G. A. Bray, *Anal. Biochem.* **1**, 279 (1960).
7. O. H. Lowry, N. J. Rosebrough, L. A. Farr, R. J. Randall, *J. Biol. Chem.* **193**, 265 (1951).
8. M. B. Glendening, A. J. Margolis, E. W. Page, *Am. J. Obstet. Gynecol.* **81**, 591 (1961).
9. A. C. Kulangara and O. A. Schjeide, *Nature* **195**, 811 (1962).
10. Aided by grants from the Charles and Marjorie King Fund and from the Association for the Aid of Crippled Children, and by training grant 2G-144 from the National Institutes of Health.

21 January 1963

Intracellular Potentials of Cortical Neurons during Focal Epileptogenic Discharges

Abstract. *Focal electroencephalographic discharges in lesions of cortex induced by freezing are associated with prolonged membrane depolarizations and hyperpolarizations in neurons located at various depths in the lesion sites. Transmembrane potential changes have properties similar to those of postsynaptic potentials. The temporal relationship between intracellular potentials and paroxysmal discharges indicates that the latter are extracellularly recorded summations of synchronously developing depolarizations and hyperpolarizations in complex synaptic organizations of neurons.*

The focal electroencephalographic spike and sharp wave represent elementary electrographic abnormalities observed in clinical electroencephalography (EEG). Although recent reviews have stressed the possible relationship of paroxysmal activities to extracellularly recorded unit discharges (*1*), we do not know to what extent the different electrical responses of neurons contribute to the production of cortical surface EEG spikes. Intracellular recording from cortical neurons has revealed membrane depolarizations and hyperpolarizations during different stages of strychnine-induced seizure discharges (*2*). These responses have been attributed to strychnine potentiation of spontaneous oscillations of membrane potential. Some temporal correlations have been noted between

hippocampal after-discharges and transmembrane potential changes in pyramidal neurons (*3*). In contrast, slow membrane depolarizations or hyperpolarizations have not been observed in neurons in chronic epileptogenic lesions resulting from intracortical injection of alumina cream (*4*).

In our study focal EEG spikes and sharp waves were produced in encéphale isolé cats by local cortical freezing in order to elicit regular low-frequency discharges with stable electrographic characteristics (*5*). The lesions produced by cold generally became epileptogenic within a few hours. When discharges were well established, lesion sites were explored with microelectrodes filled with 2*M* potassium citrate. Intracellular potentials were recorded after passage through a neutralized capacitance input d-c amplifier. Details concerning preparation of animals and recording techniques were similar to those described elsewhere (*6*).

Several types of intracellularly recorded neuronal activities were observed in association with focal EEG spikes and sharp waves. Despite the wide variation in activity from cell to cell, the pattern in a particular neuron during a stereotyped low-frequency EEG discharge was remarkably stable. Figure 1 illustrates two major types of neuronal activity from cells impaled during a single penetration of an epileptogenic focus. In one group of cells acceleration of firing was observed during different phases of the surface-negative electrocortical activity (Fig. 1*A*). Observations made at different times after impalement of such cells clearly revealed a prolonged but variable amplitude depolarization during the surface-negative phase of the cortical paroxysmal activity (Fig. 2, *A–C*). Occasionally gradual or abrupt changes in steady depolarization resulted in soma spike-inactivation. Similar observations have been made in cortical neurons treated with strychnine (*2*).

Particular importance attaches to findings that cells showing prolonged depolarizations and increased frequency of firing during EEG paroxysmal waves were frequently less than 50 μ from elements exhibiting sustained membrane hyperpolarization during the focal surface activity. Membrane hyperpolarization with cessation of firing might persist for several hundred milliseconds during all phases of the surface recorded activity (Fig. 1, *B* and *C*) or only during the initial negative component of diphasic focal discharges (Fig. 1, *D* and *E*). In many instances hyperpolarization developed simultaneously with the cortical surface negativity (Fig. 1*B*). Successive surface negativities were then accompanied by additional phases of membrane hyperpolarization (Fig. 1*C*). Less commonly, hyperpolarization preceded the onset of cortical surface negativity (Fig. 1*E*). The magnitude of the repolarizing or hy-

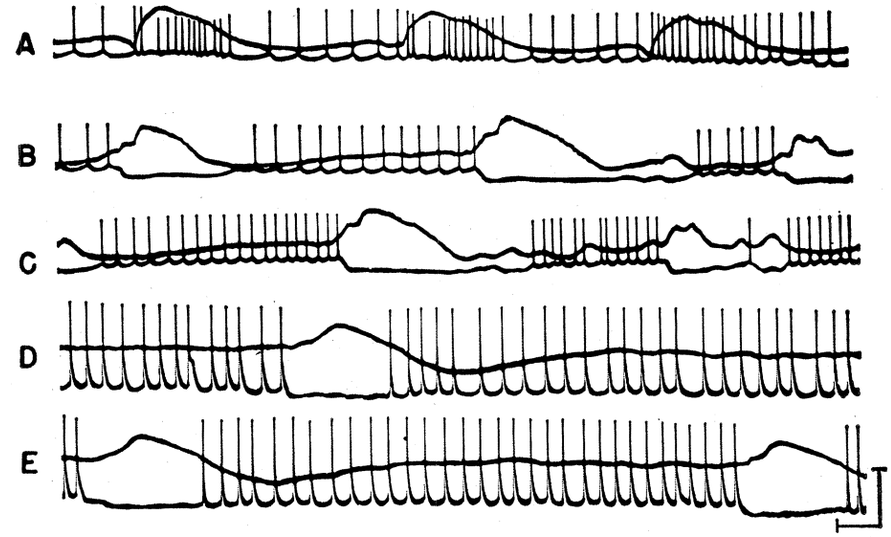

Fig. 1. Upper traces: monopolar recordings of focal surface EEG discharges in an epileptogenic lesion involving motor cortex (negativity upward). Lower traces: intracellular recordings from three neurons impaled during a single penetration of the lesion site (negativity downward). (*A*) Neuron in the cortical depths exhibiting minimal depolarization and acceleration of firing during surface negativity. (*B* and *C*) Continuous recording from another cell approximately 50 μ above the neuron shown in *A*. Membrane hyperpolarization with inhibition of cell discharge is evident during all phases of EEG paroxysmal waves. (*D* and *E*) Continuous recording from cell superficial to that shown in *B* and *C*. Inhibition of cell discharge occurs only during surface negativity of diphasic low-frequency EEG paroxysmal activity. Calibrations: horizontal bar, 0.1 second; vertical bar, 0.5 mv for surface EEG traces and 50 mv for intracellular records.

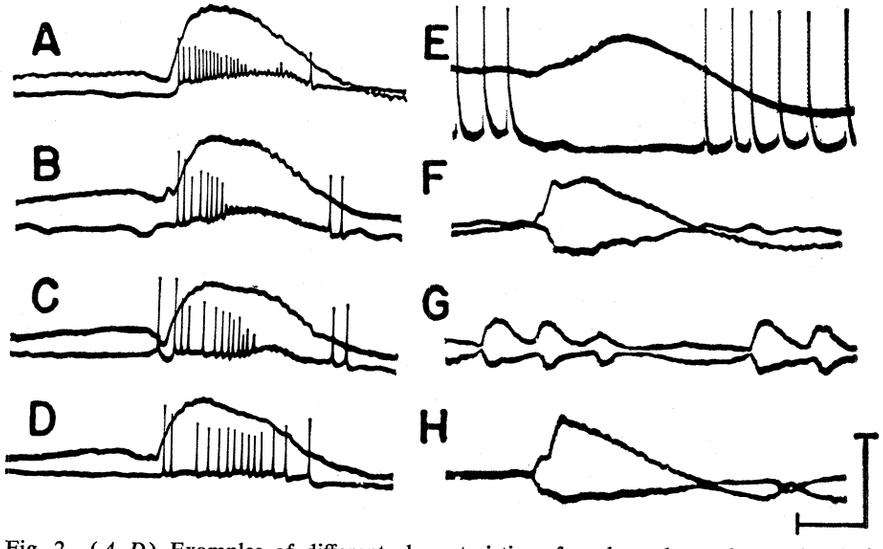

Fig. 2. (*A–D*) Examples of different characteristics of prolonged membrane depolarizations in the same cell during the course of continuous recording of EEG-discharge shown in Fig. 1*A*. (*E-H*) Relationship of hyperpolarizations to membrane potential level in another cell. (*E*) Cell in condition similar to that shown in Fig. 1*D*. (*F*) Several seconds after loss of spike-generating mechanism subsequent to progressive deterioration. Cell depolarized 30 mv below level shown in *E*. Despite severe depolarization prominent repolarizing potentials are generated during focal EEG activity. Note in *G* and *H* the close correlation between different characteristics of EEG discharge and membrane potential changes. Calibrations: same as in Fig. 1.

perpolarizing potentials was related to the degree of depolarization produced by background excitatory synaptic bombardment or injury. Cells with 60 to 70 mv spikes exhibited minimum (3 to 5 mv) hyperpolarizations during paroxysmal EEG waves, whereas larger polarizing potentials (10 to 15 mv) were recorded in slightly depolarized cells with 40 to 50 mv spikes. Deteriorating cells depolarized to the level of spike inactivation exhibited augmented repolarizing potentials. In such neurons membrane repolarizations during the EEG spikes had a time-course similar to the hyperpolarizations observed prior to spike inactivation (Fig. 2, *E* or *F*). Changes in frequency and duration of surface EEG spikes or sharp waves were associated with parallel changes in repolarizing potentials (Fig. 2, *G* and *H*).

Our study establishes that EEG spikes or sharp waves are temporally related to synchronously developing membrane depolarizations and hyperpolarizations in neurons in epileptogenic foci. Depolarizations may or may not be associated with all-or-none discharges, whereas hyperpolarizations invariably produce inhibition of firing. The characteristics of these membrane potential changes are similar to those of prolonged postsynaptic potentials. This is particularly evident with respect to the hyperpolarizations or repolarizations which survive loss of the spike-generating mechanism and exhibit a relationship to membrane potential level expected for inhibitory postsynaptic potentials (*7*).

Although prolonged membrane potential changes and EEG discharges are closely related temporally, their relation with respect to polarity is variable as in the case of hippocampal seizure activities (*3*). The EEG spike or sharp wave in a lesion produced by freezing is a reflection of the sum of membrane depolarizations and hyperpolarizations in neurons located at various depths. Thus the polarity of the focal EEG discharge appears to be a consequence of variations in the magnitude and proportion of depolarizing, excitatory, and hyperpolarizing, inhibitory postsynaptic potentials generated in neurons in complex synaptic organizations (*8*, *9*).

ELI S. GOLDENSOHN
DOMINICK P. PURPURA
Departments of Neurology and
Neurological Surgery, College of Physicians and Surgeons, Columbia University, New York 32

References and Notes

1. J. K. Merlis, in *Neuronal Physiopathology*, R. G. Grenell, Ed. (Harper and Rowe, New York, 1962); A. A. Ward, Jr., in *Intern. Rev. Neurobiol.* **3**, 137 (1961).
2. C. L. Li, *J. Neurophysiol.* **22**, 436 (1959).
3. E. R. Kandel and W. A. Spencer, *Exptl. Neurol.* **4**, 162 (1961).
4. J. R. Atkinson, J. M. Macs, A. A. Ward, Jr., *Electroencephalog. Clin. Neurophysiol.* **13**, 824 (1961).
5. T. G. Smith, Jr., and D. P. Purpura, *ibid.* **12**, 59 (1960).
6. D. P. Purpura and B. Cohen, *J. Neurophysiol.* **25**, 621 (1962).
7. J. C. Eccles, *Ergeb. Physiol. Biol. Chem. Exptl. Pharmakol.* **51**, 299 (1961); H. Grundfest, in *Handbook of Physiology, Neurophysiology*, J. Field, Ed. (American Physiological Society, Washington, D.C., 1959), vol. 1, p. 147.
8. D. P. Purpura, *Intern. Rev. Neurobiol.* **1**, 47 (1959).
9. Supported in part by the National Institute of Neurological Diseases and Blindness (B 1312-C5) and the United Cerebral Palsy Research and Education Foundation (R-135-62 C). One of us (E.S.G.) is a career research scientist, New York City Health Council; the other (D.P.P.) is a research career development fellow, National Institute of Neurological Diseases and Blindness.

24 December 1962

Xenon Difluoride and the Nature of the Xenon-Fluorine Bond

Abstract. *Xenon reacts with fluorine to form XeF_2 which can be isolated before it reacts with fluorine to form XeF_4. The linear configuration of XeF_2 with the 2.00-A bond length and the vibrational force constants support the assignment of 10 electrons to the valence shell of xenon. Similar arguments support the assignment of 12 and 14 valence electrons respectively to xenon in XeF_4 and XeF_6.*

In their report on XeF_4, Claassen, Selig, and Malm (*1*) noted a lower fluoride, which was identified by Chernick *et al.* (*2*) as XeF_2. Smith's study (*3*) of the xenon-fluorine reaction resulted in a method of preparation of nearly pure XeF_2. The molecular configuration, the Xe-F bond distance, and the vibrational force constants have been obtained from x-ray (*4*) and neutron (*5*) diffraction and from infrared and Raman spectra (*6*), and have led to some understanding of the nature of the Xe-F bond.

The loop used to study the Xe-F_2 reaction is shown in Fig. 1. The loop provides for examination of the infrared spectrum of the reaction mixture to determine composition or production rates. The circulating gas passes rapidly through the short hot zone where the reaction

$$Xe + F_2 \rightarrow XeF_2 \qquad (1)$$

occurs with a rate increasing as the partial pressure of Xe or F_2 is increased. XeF_4 is produced only when XeF_2 reacts with F_2,

$$XeF_2 + F_2 \rightarrow XeF_4. \qquad (2)$$

The rate of Reaction 2 increases as the partial pressure of XeF_2 or F_2 is increased. Both reactions go faster as the temperature is increased. Reaction products were observed at temperatures as low as 270°C. Reaction 2 produces little XeF_4 if the reaction rates are kept low and if the XeF_2 is trapped out before it passes into the reaction zone. With care, nearly pure XeF_2 has been obtained. These conditions were satisfied by Weeks *et al.* (*7*) in their photochemical preparation of XeF_2, while the reaction described by Claassen *et al.* (*1*) resulted in pure XeF_4 because the XeF_2 produced was retained in the closed reaction vessel with F_2 until it all reacted.

Xenon difluoride is remarkably similar to and difficult to separate from XeF_4. It is a solid with a vapor pressure of 3.8 mm-Hg at 25°C and 318 mm-Hg at 100°C. It forms clear, brilliant crystals that grow to millimeter dimensions in a few hours. The solid melts at about 140°C and can be supercooled as much as 50°C without solidifying.

Two intense infrared bands in XeF_2 vapor have been observed at 555 cm^{-1} and 213.2 cm^{-1}. The first, with no *Q* branch, has been assigned as ν_3 (asymmetric stretching) and the second, with a well defined *Q* branch, as ν_2 (bending). A third band observed at 1070 cm^{-1} is the weak combination band $\nu_1 + \nu_3$, from which the infrared inactive vibration ν_1 may be obtained as 515 cm^{-1}. Band contours are characteristic of a linear symmetrical molecule. The *P-R* separation of ν_3, 16 cm^{-1}, is inversely proportional to the square root of the moment of inertia and yields an estimate of 1.7 A for the Xe-F distance, in accord with the more precise value obtained by diffraction. Raman lines for solid XeF_2 were found at 108 cm^{-1} (intensity, 0.33), 497 cm^{-1} (intensity, 1.00), 548 cm^{-1} (intensity, 0.07), with an indication of another at 509 cm^{-1}. The first is probably a libration frequency; the second is clearly ν_1, and the other two are ascribable to an impurity of XeF_4. The fundamental frequencies for the vapor yield the following force constants (in millidynes per angstrom): k, (principal stretching constant), 2.85; k_{rr} (stretch-